Understanding the kinetics of spin-forbidden chemical reactions

Jeremy N. Harvey*

Received 3rd October 2006, Accepted 2nd November 2006
First published as an Advance Article on the web 20th November 2006
DOI: 10.1039/b614390c

Many chemical reactions involve a change in spin-state and are formally forbidden. This article summarises a number of previously published applications showing that a form of Transition State Theory (TST) can account for the kinetics of these reactions. New calculations for the emblematic spin-forbidden reaction HC + N_2 are also reported. The observed reactivity is determined by two factors. The first is the critical energy required for reaction to occur, which in spin-forbidden reactions is often defined by the relative energy of the Minimum Energy Crossing Point (MECP) between potential energy surfaces corresponding to the different spin states. The second factor is the probability of hopping from one surface to the other in the vicinity of the crossing region, which is largely defined by the spin–orbit coupling matrix element between the two electronic wavefunctions. The spin-forbidden transition state theory takes both factors into account and gives good results. The shortcomings of the theory, which are largely analogous to those of standard TST, are discussed. Finally, it is shown that in cases where the surface-hopping probability is low, the kinetics of spin-forbidden reactions will be characterised by unusually unfavourable entropies of activation. As a consequence, reactions involving a spin-state change can be expected to compete poorly with spin-allowed reactions at high temperatures (or energies).

1. Introduction

One of the most exciting developments in computational chemistry is the ability to predict the rate coefficients of chemical reactions. For relatively small gas-phase species, mostly reactions involving three or four atoms only, it is possible to calculate a full-dimensional potential energy surface and solve the scattering problem exactly using time-independent or time-dependent (wave-packet) methods.[1] These methods can also be extended to systems with more atoms, either by treating some 'spectator' degrees of freedom in a more approximate way,[2] or by using sophisticated interpolation methods for the potential energy surface and the multi-configurational time-dependent Hartree product method to propagate wavepackets.[3] In all these cases, provided the electronic structure calculations on the potential energy surfaces are accurate enough (*e.g.* barrier heights to within better than 1 kcal mol^{-1}) then rate coefficients can be determined with an accuracy approaching or indeed exceeding that of experiment.

For larger systems, especially those in which it is not straightforward to separate 'active' and 'spectator' degrees of freedom, this type of approach remains impossible, but very accurate results can be obtained using modern versions of Transition State Theory (TST),[4] including such effects as tunneling and variational optimization of the position of the transition state. These methods even yield good results for very challenging problems such as calculating rate coefficients[5] and isotope effects[6] for enzymatic reactions. In fact, for many reactions, even the simplest form of TST gives reasonably good results (rate coefficients within one order of magnitude of experiment), provided that care is taken to calculate the barrier height accurately.[7] Despite extensive debate on the applicability of TST due to effects such as non-ergodicity, barrier recrossing or solvent friction,[8] this theory clearly has enormous predictive power.

Perhaps an even more important contribution of TST is that it provides a fundamental framework in which to think about the rate coefficients of chemical reactions. The activation enthalpy is a quantity that is readily understood in terms of the same criteria of bonding and steric effects that are commonly used by chemists when designing new compounds. This means that for two similar reactions, chemists will often be able to predict the difference in activation enthalpy from rough knowledge of the geometry and bonding character of the transition state. The activation entropy is perhaps less well understood, but can likewise be rationalised and predicted based on the 'looser' or 'tighter' nature of the transition state, and on the number of translational and rotational degrees of freedom. In this way, when computational chemists locate a transition state, or experimental chemists propose a transition state structure, this in itself is often used to rationalise reactivity by an *implicit* reference to TST.

Given this paradigmatic role of TST in understanding chemical reactivity, it is perhaps not surprising that chemists become much less confident when discussing processes to which TST cannot be directly applied. One such category of process is spin-forbidden reactions; that is, reactions in which a change of spin state occurs, and this is the topic of the present study.[9,10] These reactions are said to be *non-adiabatic*, in the sense that they occur on more than one potential energy surface, with transformation of reactants to products

Centre for Computational Chemistry and School of Chemistry, University of Bristol, Cantock's Close, Bristol, UK BS8 1TS. E-mail: jeremy.harvey@bristol.ac.uk

requiring the system to 'hop' from the potential energy surface corresponding to the initial spin state onto that corresponding to the product state for reaction to occur. In fact, in some cases, reactions may require more than one hop, for example if the mechanism involves an intermediate with a different spin state to that of both the reactants and the products. This means that a reaction can be spin-forbidden even if reactants and products have the same spin state if more than one spin change occurs.

Potential energy surfaces can be of two types: adiabatic or diabatic. Adiabatic surfaces are defined within the Born–Oppenheimer approximation by the energy (eigenvalue) of a given solution to the electronic Schrödinger equation at each geometry. Such solutions are obtained by using the *full* electronic Hamiltonian, that is, including kinetic energy, Coulomb, scalar relativistic and spin–orbit terms. Diabatic surfaces can be defined as generated from the eigenvalues of the Schrödinger equation solved using a Hamiltonian from which one or more terms have been omitted; in the present case, the spin–orbit coupling terms. Surfaces of both types are shown for a notional spin-forbidden reaction in Fig. 1. Reactants are on diabatic surface 1 (*e.g.* corresponding to a triplet state), with products on surface 2 (*e.g.* a singlet). The corresponding minima have different geometries, and the surfaces cross at the Minimum Energy Crossing Point (MECP).

The adiabatic surfaces A and B in Fig. 1 do not cross, as the spin–orbit coupling matrix element $H_{12} = \langle \Psi_1 | H_{soc} | \Psi_2 \rangle$ is non-zero and, therefore, when H_{soc} is included in the Hamiltonian, the eigenfunctions are mixtures of different spin states. This means that, in principle, there is a well-defined transition state on the lower surface. In extreme cases, spin–orbit coupling may indeed be so strong that the mixing takes place over a broad range of geometries around the TS, and the reaction can in fact be described in the usual way using standard TST. In practice, for very many cases, the mixing is rather weak and non-adiabatic, non-Born–Oppenheimer behaviour will occur: the system will undergo 'hops' from one surface to the other. These can be described either in terms of the diabatic surfaces, as sudden changes in spin state, or in terms of the adiabatic surfaces, as sudden hops from the lower adiabatic surface, A, to the upper one, B.

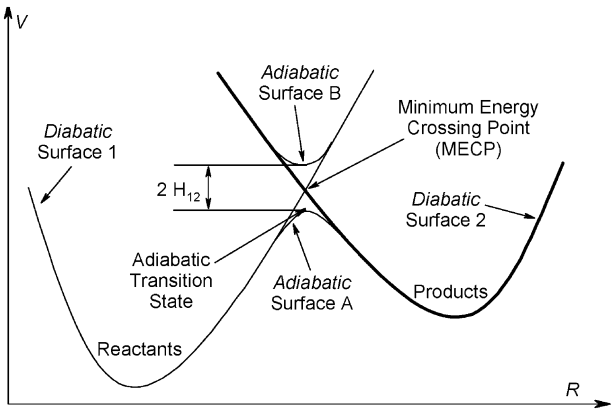

Fig. 1 Schematic diabatic and adiabatic potential energy surfaces for a spin-forbidden reaction.

For example, in the limit of very weak spin–orbit coupling, a system approaching the crossing region from the reactant side is most likely, in diabatic terms, to remain on surface 1, and then return to reactants. In adiabatic terms, when the system approaches the very narrowly-avoided crossing between surfaces A and B it will 'hop' onto the upper surface. Upon returning from right to left on the diagram, it will hop again at the avoided crossing, back onto surface A and thereby head back to reactants. These two descriptions are equivalent, with the second perhaps more natural to theoretical chemists, but with the first more convenient for our purposes. We will therefore use the diabatic framework throughout. In this terminology, for reaction to occur, spin–orbit coupling must induce a 'hop' from surface 1 to surface 2 as the system goes through the crossing region. Hops can occur at any position along the reaction coordinate, but are more likely in the small region around the crossing point where the two surfaces are close in energy.

2. Non-adiabatic transition state theory

The preceding discussion suggests a model for understanding chemical reactivity in spin-forbidden reactions. First, the system needs to access the crossing seam between the potential energy surfaces corresponding to the different spin states, and this will lead to an activation energy for the reaction. Next, the system needs to hop from one diabatic surface to the other in the region surrounding the seam, which requires spin–orbit coupling between the surfaces. This is the model we have used in our previous studies of spin-forbidden processes and again in this paper.

This model has in fact been used for some time, for example, in a number of studies of O (^{1}D) quenching by N_2.[11,12] It has also been incorporated into a form of non-adiabatic transition state theory.[13] We recently adapted this non-adiabatic TST both for unimolecular reactions in a microcanonical form[14] and for bimolecular reactions in a canonical form.[15] The unimolecular microcanonical form gives the expression shown in eqn (1) for the rate coefficient $k(E)$ of a spin-forbidden reaction at a given internal energy E:

$$k(E) = \frac{N_{cr}(E)}{h\rho(E)} \quad (1)$$

$$N_{cr}(E) = \int \mathrm{d}E_h \rho_{cr}(E - E_h) p_{sh}(E_h) \quad (2)$$

In eqn (1), $\rho(E)$ is the density of rovibrational states of the reactant. $N_{cr}(E)$ is the effective integrated density of states in the crossing seam between the two surfaces. As in simple TST, this integrated density of states is derived by assuming that the motion of the system can be divided into two distinct types that are not coupled in the vicinity of the crossing. The first type of motion is along the single degree of freedom orthogonal to the crossing seam, or 'hopping' coordinate (R in Fig. 1), while the second is motion parallel to the crossing seam, in the 'spectator' rotational and vibrational degrees of freedom (orthogonal to the plane of Fig. 1). N_{cr} is therefore given as an integral (2), a convolution of the probability of hopping from one surface to another for a given amount of energy in

the hopping coordinate, $p_{sh}(E_h)$, with the density of rovibrational states in the 'spectator' degrees of freedom, $\rho_{cr}(E–E_h)$, corresponding to the remaining energy.

The probability of hopping p_{sh} can be calculated from Landau–Zener theory[16,17] as shown in eqn (3):

$$p_{sh}(E) = (1 - P_{LZ})(1 + P_{LZ})$$
$$\text{where } P_{LZ} = \exp\left(\frac{-2\pi H_{12}^2}{\eta \Delta F}\sqrt{\frac{\mu}{2E}}\right) \quad (3)$$

In this equation, H_{12} is the spin–orbit coupling-derived off-diagonal Hamiltonian matrix element between the two electronic states, and ΔF is the relative slope of the two surfaces at the crossing seam. The reduced mass of the system as it moves along the hopping coordinate is μ, and E is the kinetic energy of the system as it passes through the crossing seam. Note that this means that $p_{sh}(E_h)$ in eqn (1) should strictly be given as $p_{sh}(E_h–E_c)$, where E_c is the energy of the MECP relative to the reactants. P_{LZ} gives the Landau–Zener probability for hopping from one *adiabatic* state (Fig. 1) to another during a single pass through the crossing region. We are interested in the probability of hopping from one diabatic state to the other during a potential double pass through the crossing region, and this is given by $(1 - P_{LZ})$ (the probability of hopping on the first pass) plus $P_{LZ}(1 - P_{LZ})$ (the probability of not hopping on the first pass, then hopping on the second pass).

The Landau–Zener form eqn (3) of the hopping probability is equal to zero for energies below the MECP, *i.e.* when E_h is smaller than E_c. Another expression has been suggested[11] that allows for tunneling at energies below the MECP, as shown in eqn (4).[18] In this expression, F is the average of the slopes on the two surfaces, Ai denotes the Airy function, and H_{12}, μ and E have the same meaning as in eqn (3).

$$p_{sh}^{tunnel}(E) = 4\pi^2 H_{12}^2 \left(\frac{2\mu}{\eta^2 F \Delta F}\right)^{2/3} Ai^2\left[-E\left(\frac{2\mu\Delta F^2}{\eta^2 F^4}\right)^{1/3}\right] \quad (4)$$

When energy equilibration with the environment is faster than reaction, as in most bimolecular reactions or in unimolecular processes in condensed phases, a canonical expression for the rate coefficient as a function of temperature, as shown in eqn (5), is preferable to the microcanonical eqn (1):

$$k(T) = \frac{1}{hQ_R(T)} \int_0^\infty N_{cr}(E)\, e^{-E/k_B T} \mathrm{d}E \quad (5)$$

where $Q_R(T)$ is the partition function for the reactant(s), as a product of rotational, vibrational and (for bimolecular reactions) relative translational terms. N_{cr} is given by eqn (2), and is convoluted with a Boltzmann factor so as to average over the different reactant energies.

To apply this theory, it is necessary to be able to locate and characterize the region where the potential energy surfaces cross. One convenient way to do this is to locate the lowest energy point within the crossing seam, or MECP.[19] This point can be located using a simple minimization procedure,[20,21] by following the effective gradient $\alpha\nabla(V_1–V_2)^2 + \mathbf{P}(\nabla V_1)$, where V_1 and V_2 are the potential energies on the two surfaces and α is an arbitrary coefficient, which for efficiency is chosen so as to make the two terms of the gradient of similar magnitude. **P** denotes a projection operator which removes from the gradient on surface 1, ∇V_1, the direction corresponding to the difference in gradient on the two surfaces, $\nabla(V_1 - V_2)$. Other methods for locating MECPs have been proposed,[22] using Lagrangian multipliers or other approaches.

Alternative ways to locate the crossing region between potential energy surfaces have been suggested and used in a number of cases. One of the most common is what we have called the 'partial optimization' method.[23] This involves carrying out a set of geometry optimizations on both potential energy surfaces, with a particular internal coordinate (*e.g.*, a bond length or an angle between two bonds) constrained to have a series of different fixed values. This generates one-dimensional cuts in the two potential energy surfaces, and these cuts may cross at certain values of the chosen coordinate. This crossing point is only an approximation to the MECP, however, because the optimum value of the orthogonal degrees of freedom on the two potential energy surfaces may not be the same. This method is also more time-consuming than direct optimization of the MECP geometry, in that it involves $2N$ separate geometry optimizations (where N is the number of different frozen values of the coordinate).[23]

Because the system must undergo a non-adiabatic 'hop' at the MECP, and because the adiabatic electronic wavefunction in the region of the MECP is a mixture of different spin states, one might think at first sight that a very flexible electronic structure method is needed to locate MECPs. In particular, it might appear that only multi-reference methods such as CASSCF or MR-CI are suitable. In some cases, this is definitely true, as the electronic wavefunction of one of the states involved may have substantial multi-reference character. However, in many cases, the wavefunctions corresponding to the *diabatic* electronic states in the region of the MECP may be well described by single-reference methods, such as Density Functional Theory (DFT) or Møller–Plesset perturbation theory (MP2). In such cases, any method able to give an accurate description of the two states and of their relative energy will be suitable for locating the MECP.[24] This is the case for all the systems described below (except perhaps for the dissociation of N_2O, but in that test case we used analytical expressions to describe the two potential energy surfaces).

The MECP provides a natural choice for the hopping coordinate, as the gradients on the two surfaces at the MECP are either parallel or antiparallel, and are orthogonal to the seam of crossing. Within the seam, the MECP is a minimum, and it is possible to calculate vibrational frequencies for the spectator modes,[21] which, together with the structure and hence rotational constants, enables one to calculate the rovibrational densities of states $\rho_{cr}(E)$. To calculate the probability of surface hopping, it is assumed that the two surfaces can be expanded using a first-order Taylor expansion along the hopping coordinate in the vicinity of the MECP, and that the spin–orbit coupling element H_{12} does not vary significantly around the MECP.

We[14] as well as others[25] have shown how the properties of the MECP can be used in this way to calculate rate coefficients for spin-forbidden reactions. In the present paper, we will review some of these applications, present some new results,

discuss the accuracy of the method, and the kinetic behaviour of spin-forbidden reactions.

3. Qualitative applications

Although it is relatively straightforward to apply the non-adiabatic TST described above in eqn (1) and (4), in many cases this is not very useful, and we have simply used the properties of the MECP to make qualitative predictions of reactivity. The reason for this is that the predicted rate coefficient is very sensitive to the height of the reaction barrier, that is, to the relative energy of the MECP. With typical computational methods, the error on this relative energy is expected to be up to 5 kcal mol^{-1}, which would lead to errors on the calculated rate coefficient at room temperature of several orders of magnitude. However, when comparing the height of MECPs corresponding to two different reactions, or the relative energy of an MECP with that of an adiabatic TS for a competing process, the error is likely to cancel out somewhat, and qualitative predictions of reactivity can be made.

We have studied a number of reactions and used the properties of the MECP to reach such qualitative conclusions. Although some of our work has addressed chemistry of main-group compounds,[26] we have mainly focussed on transition-metal-containing systems.[9,23,27] The focus of the present paper is on quantitative applications of non-adiabatic TST, so this work will not be discussed further here.

It is, however, important to note that as MECPs are located for more and more systems, it starts to become possible to make generalizations concerning the relation between the nature and shape of the individual potential energy surfaces, the topology of the surface crossing, and the relative energy of the MECP. With more experience, it may become possible to make reasonably accurate guesses about the energy of MECPs, and hence about spin-forbidden reactivity, simply based on analogy to other systems. This type of reasoning is extremely common for normal, spin-allowed reactions, and it would be very advantageous if it became possible for spin-forbidden processes.

A number of such observations have already been made. First, it has been observed that the MECPs between two different spin states of the same chemical species tend to be located fairly close in geometry and in energy to the minimum of the higher-lying state.[27b,28] This is presumably due to the fact that the geometry of the two minima are fairly similar, so that a relatively small distortion of the lower state is enough to cause a crossing of the two surfaces. Another observation is specific for transition metal chemistry: many spin-forbidden processes in that area involve unsaturated triplet states with a formal electron count of 16, and the MECP occurs upon addition of an extra ligand, leading to a singlet 18-electron species. The MECP will usually lie lower in energy than the 16-electron fragment provided the approach of the extra ligand causes a lowering of the energy on the triplet surface. This will tend to occur when the incoming ligand is stronger-field than the existing ligands, *e.g.*, when the incoming ligand is CO, and ligands already in place are weaker-field. In contrast, weaker incoming ligands, such as N_2 or H_2 will not lead to an attractive interaction on the high-spin surface, so the MECP will tend to lie higher than the separated fragments. A number of examples where this rule applies have been described.[27b,29] Finally, it has been observed[26b,27a] that for homologous reactions, an analogue of Hammond's postulate applies, so that a more exothermic reaction step correlates with an MECP that is both 'earlier' (more similar to the reactants) and lower in energy.

4. Quantitative applications

In this section, we summarise the results of some applications of spin-forbidden TST, focussing primarily on our own results.[30] We also present, in detail, new results obtained for the HC + N_2 reaction.

(a) Predissociation of N_2O

The lowest energy dissociation pathway for singlet N_2O leads to triplet (N_2 + O) fragments. The singlet and triplet surfaces cross at an MECP lying roughly 60 kcal mol^{-1} above the singlet minimum, as shown in Fig. 2. Many studies (not all cited here) have addressed the spin-forbidden processes involving these two electronic states.[11,12,31,32] We used the predissociation reaction of N_2O to give N_2 and O (^{3}P) as a first test of the accuracy of the spin-forbidden TST method.[14] Our calculated microcanonical rate coefficients for dissociation show the two effects mentioned above. First, no reactivity is observed below the threshold energy, defined by the height of the MECP. Next, the rate coefficient even at high energies is only in the range of 10^{11} s^{-1}, somewhat smaller than it would be for an analogous spin-allowed process, due to the requirement for spin-hopping.

Our results agree to within much less than one order of magnitude with those obtained by Marks and Thompson[31] using either non-adiabatic Monte Carlo phase-space theory or surface-hopping classical trajectories. In turn, these results were also similar to those obtained using quantum dynamical calculations.[33] This quantitative agreement of the simple TST with more accurate (but more time-consuming) methods is very encouraging.

(b) Dissociation of CH_3O^+

The methoxy cation CH_3O^+ has a triplet ground state. When formed in the source of a mass spectrometer, it dissociates readily to give H_2 and the formyl cation, HCO^+. As the products both have singlet ground states, this is a spin-forbidden reaction. One possible mechanism for the dissociation is initial spin-forbidden isomerisation to the singlet

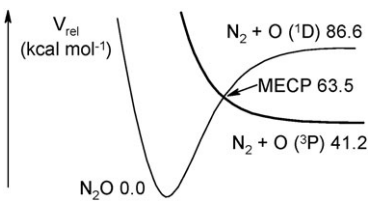

Fig. 2 Schematic singlet and triplet potential energy surfaces for N_2O, using the parameters of ref. 12*b* (MECP energy from ref. 14).

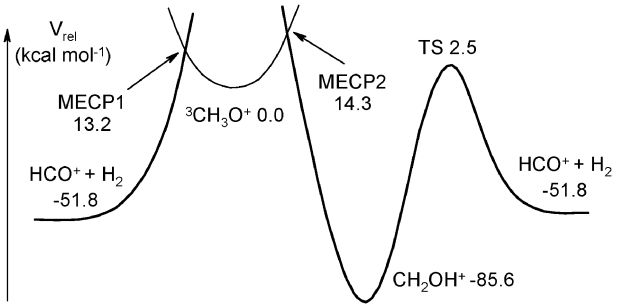

Fig. 3 Schematic calculated[14,34] (CCSD(T)/cc-pVTZ//B3LYP) triplet and singlet potential energy surfaces for decomposition of CH_3O^+.

hydroxymethyl cation CH_2OH^+, which is known to undergo metastable decomposition to give the same HCO^+ ion.

An experimental study[34] on decomposition of the different isotopomers $CH_{3-x}D_xO^+$ (x = 0–3) showed that this two-step mechanism is not consistent with the observed isotope effect on decomposition, which suggests instead a concerted mechanism. Calculations[34] (Fig. 3) show that the triplet surface intersects with the singlet surface at two low-lying MECPs.[35] The second of these, MECP2, leads to isomerisation to the hydroxymethyl cation. However, the other, MECP1, leads to direct loss of hydrogen, and lies slightly lower in energy.

Non-adiabatic TST calculations[14] of the energy-dependent rate coefficient for dissociation along both pathways support a larger rate for the direct pathway. These calculations also qualitatively reproduce the observed[34] isotope effect for dissociation of the mixed isotopomers $CH_{3-x}D_xO^+$ (x = 1, 2), which is mainly attributed to the difference in zero-point energy at the isotopomeric MECPs.

In this case, no experimental or higher level theoretical data is available concerning the value of the dissociation rate coefficient as a function of internal energy. This makes it impossible to assess the absolute accuracy of the theory used. However, indirect evidence concerning the rate of decay is available from the fact that the methoxy cation is extremely difficult to generate using most ionisation methods. This suggests that decay is rapid on the timescale of the residence time in a typical mass spectrometer. The ions in the experimental study discussed here[34] were generated by charge reversal of the corresponding anion,[36] which is a relatively soft method generating ions with low internal energies. The ions are observed to undergo decay to HCO^+ and H_2 on the microsecond timescale. The calculations predict that even ions with an energy as much as 10 kcal mol^{-1} below the classical threshold defined by the height of the MECPs dissociate on this timescale, due to tunneling from one surface to the other. This shows that the methoxy cation is an intrinsically unstable species, and hence explains why it is so difficult to generate in mass spectrometers.

(c) Radiationless transitions in triplet norbornene

Spin-state changes as well as other non-adiabatic processes are known to occur frequently in photochemistry. In many cases, the focus of interest is on the rapid events occurring after excitation to the Frank–Condon region, with the initial wavepacket undergoing movement through conical intersections to lead to different excited states, including, in some cases, triplet states. To rationalise such phenomena, an intrinsically dynamical method may be needed, or at least a map of the whole potential energy surface along key coordinates.[37] The statistical method discussed here is only suitable for slower processes occurring after the molecule has undergone a few vibrations on the excited state surface and vibrational energy has been distributed throughout the molecule. The temperature-dependent rate expression of eqn (5) is meaningful only after collisions with bath gas or solvent have removed excess internal energy from the initially formed states. However, relatively slow spin-forbidden inter-system crossing of this type is fairly common, and we have studied one reaction of this type.

The T_1 first triplet excited state of norbornene undergoes non-radiative decay to the ground state, with a timescale of *ca.* 250 ns.[38] Although this process is quite fast, it is slow enough to imply substantial vibrational energy redistribution after formation of the triplet, so that a statistical treatment of the decay is appropriate. The small lifetime of the triplet is consistent with our finding[39] that the MECP between the S_0 and T_1 states lies just 8.1 kcal mol^{-1} above the minimum of the triplet excited state at the CASSCF level of theory. Spin–orbit coupling at the MECP between the two states is rather weak, at only 0.7 cm^{-1}, but this is enough to lead to a predicted rapid decay, with a lifetime of *ca.* 3000 ns, in acceptable agreement with experiment.

(d) Carbon monoxide addition to $Fe(CO)_4$

One of our main interests is the prediction of reactivity patterns in spin-forbidden reactions of transition metal compounds.[9] Ideally, we would like to be able to predict rate coefficients for such reactions using non-adiabatic transition state theory. In most cases, this is not possible due to the difficulties associated with calculating accurate potential energy surfaces for transition metal species. In one case, however, we have made considerable progress towards calculating accurate rate coefficients, and this provides valuable support for the general model, whereby reactivity is determined by the relative energy of the MECP and by the strength of spin–orbit coupling.

Carbon monoxide adds to triplet iron tetracarbonyl to provide singlet iron pentacarbonyl. This reaction, as well as a number of analogous processes, has been studied in the gas phase using infrared spectroscopic methods by Weitz *et al.*[40] More recently, some of these reactions have also been studied in solution,[41] including supercritical argon and xenon.[42] Although iron tetracarbonyl is coordinatively unsaturated and adds CO, as well as other ligands, exothermically, these addition reactions are noticeably slower than the gas-phase collisional rate or the solution diffusion rate.

Our calculations[15] show that the topology of the potential energy surfaces is very similar to that shown in Fig. 2 for N_2O: the triplet ground state of $Fe(CO)_4$ is repulsive towards CO, whereas the excited singlet state is attractive. There is an MECP lying just above the energy of the triplet reactants. The calculated rate coefficient at room temperature is in

reasonable agreement with the experimental value.[40] Two factors account for the difference between the expected gas-phase collisional rate coefficient for reactions of this type and the observed value. First, the small barrier introduces an activation energy. Next, although there is significant spin–orbit coupling between the singlet and triplet states (the coupling matrix element is of 66 cm^{-1}), the reaction is still very much in the non-adiabatic regime, with an average hopping probability of only about 0.05. These two factors—the barrier height and the spin–orbit coupling—contribute about equally to slowing this reaction.

In further work on these reactions, we are currently attempting to account for the observed reactivity in addition of other ligands. As a first step, this has required extremely high-level calculations to probe the energy difference between the singlet and triplet states of $Fe(CO)_4$.[43]

(e) Carbon monoxide geminate recombination in myoglobin

Spin-forbidden reactions play an important role in a number of bioinorganic processes. For some time, we have been interested in the reaction of small ligands with the haem group in proteins such as myoglobin. Deoxy-haem contains a penta-coordinate high-spin (quintet) ferrous iron centre, whereas addition of a ligand such as CO leads to a hexacoordinate, low-spin, iron. Photolysis of the Fe–C bond in this carbon-monoxy state is followed by relaxation to the quintet state, with the CO ligand trapped in a small pocket within the protein above the haem group. This so-called geminate pair can then either undergo geminate recombination, in which the CO rebinds to iron, or the CO ligand can diffuse through the protein out into solvent. The latter process can compete because recombination involves a barrier, due to the fact that the quintet and singlet surfaces cross at an MECP which lies above the energy of the separated high-spin fragments. In the model system shown in Fig. 4, the barrier to recombination is calculated[44] to be of 2.6 kcal mol^{-1}.

A version of eqn (5) can be used to compute the rate coefficient for geminate recombination of CO with the haem group,[45] and the results are also shown in Fig. 4. The TST description of geminate recombination requires some care, as this is formally a unimolecular process, yet the CO reactant is not chemically bound to the protein and can rotate and translate relatively freely within the pocket. Our calculations treat the CO fragment as freely rotating but its translational partition function is described using the particle in a box model, and are thereby necessarily somewhat approximate. Nevertheless, reasonable choices for the parameters in this model yield good agreement with experiment for the overall rate coefficient at room temperature.[45]

The calculations lead to two interesting observations. First, when using eqn (4) for the surface-hopping probability, the fall-off of the rate coefficient at lower temperature becomes much less steep, suggesting extensive tunneling at these temperatures, as is found experimentally.[46] Next, the reaction is quite strongly spin-forbidden: the hypothetical adiabatic rate coefficient calculated assuming that surface-hopping at the MECP occurs with unit probability is very much larger than the full, non-adiabatic rate coefficient.

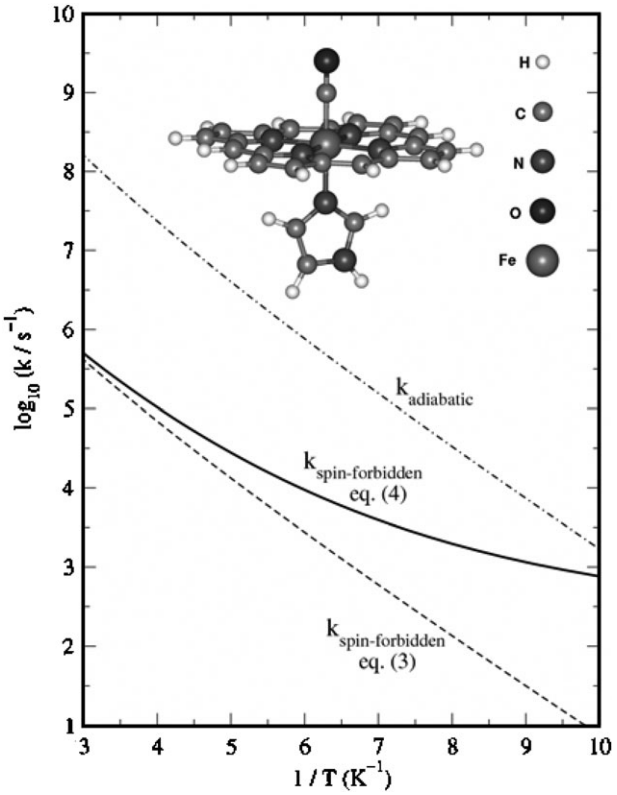

Fig. 4 Calculated spin-forbidden rate coefficients for CO geminate recombination in myoglobin showing the model system on which calculations were carried out. Results based on surface-hopping probabilities p_{sh} calculated using eqn (3) and (4) are shown separately, as well as the hypothetical rate coefficient $k_{adiabatic}$ obtained by assuming that p_{sh} is equal to 1. (Adapted from ref. 45).

(f) The reaction HC + N_2

The reaction of the HC radical with dinitrogen leading to HCN and a nitrogen atom (eqn (6)) was proposed to play an important role in the chemistry of flames. The product N atom can react with dioxygen to form 'prompt' NO. Reaction (6) is spin-forbidden because HC has a doublet ground state, whereas N has a ^4P_u ground state and N_2 and HCN are closed-shell singlet species. The overall reaction leading to NO has been the subject of extensive experimental study, so that the rate coefficient is known fairly accurately over a range of relevant temperatures. It should, however, be noted that some uncertainty remains over the nature of the intermediate species leading to NO, as the experiments do not directly monitor the formation and decay of the N atoms.

$$^2HC + ^1N_2 \rightarrow ^1HCN + ^4N \qquad (6)$$

This reaction has also received considerable attention from theoreticians. A number of groups have characterized the potential energy surfaces (Fig. 5).[47,48] Barrierless addition leads to a roughly linear doublet adduct, HCNN, but this cannot lead to products. Instead, addition over a low barrier TS1 (and through a shallow intermediate of lower symmetry) leads to a C_{2V} adduct with an NCN three-membered ring, $^2HCN_2$. The unpaired electron in this species is mainly located

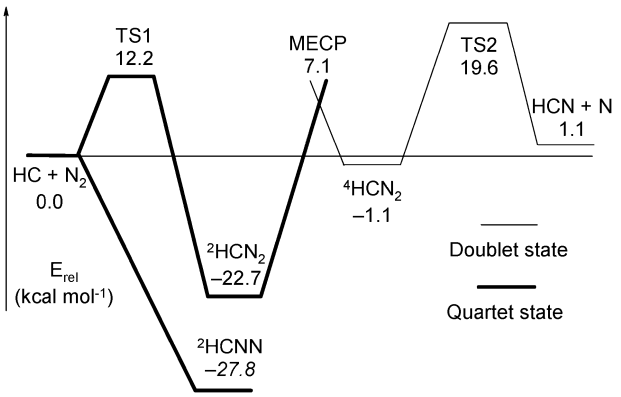

Fig. 5 Calculated potential energy surfaces for reaction (6). The energy for the HCNN adduct is taken from ref. 47 and obtained at the G2M(RCC) level; other values were obtained in this work at the CCSD(T)/cc-pVQZ//B3LYP/6-311G* level.

on the carbon atom. Opening of the NCN angle leads to an increase in energy of this doublet state, but to a stabilization of a quartet state in which the N–N bond is broken, and the three unpaired electrons are delocalized over the two nitrogens. These states therefore cross, and there is an MECP lying a few kcal mol^{-1} above a new quartet intermediate, $^4HCN_2$. The latter can then undergo dissociation over a relatively high barrier TS2 to form the products, a nitrogen atom and HCN.

Various attempts have been made to calculate rate coefficients based on these potential energy surfaces. It has been found that experimental rate coefficients can be reproduced by a relatively simple TST model using a single barrier with a height and properties similar to those calculated for TS2.[49] It was argued in this study that the MECP could not affect the rate, because reactive flux is dominated by systems having an energy lying just above the energy threshold for reaction. The latter is clearly determined by TS2, and the authors suggested that the rate of spin-state interconversion between $^2HCN_2$ and $^4HCN_2$ at the threshold energy would be much higher than the rate of barrier crossing, so that the latter would be rate determining.

In contrast to this, a NA-TST treatment very similar to that discussed above, treating the effect of TS1, TS2 and the MECP in an integrated way, and using very accurate potential energy surfaces,[47] concludes that the MECP is rate-determining, but leads to calculated rates well below experimental values.[25] Quantum dynamical calculations[50,51] of the cumulative reaction probabilities and rate coefficient using reduced-dimensionality potential energy surfaces also lead to a predicted rate well below what is experimentally observed. It is useful to examine why this is so, given that TS2 is so much higher in energy than the MECP, making the argument exposed in the previous study[49] so appealing. To do so, we have carried out our own NA-TST calculations, which we report here for the first time, and analyze the factors determining the magnitude of the rate coefficient.

First of all, we have reoptimized the geometry of the various stationary points. Previous work has shown that the geometries are not very sensitive to the level of theory used, so we have applied the B3LYP hybrid density functional method[52] and the flexible 6-311G* basis.[53] These calculations were carried out using the Gaussian program package.[54] Next, we have computed single-point energies at the ROCCSD(T) level of theory,[55] with the MOLPRO program package.[56] Calculations were carried out using the cc-pVQZ basis set,[57] with additional test calculations carried out using the smaller cc-pVTZ basis. These calculations show good convergence with respect to basis set size: for example, the quartet $^4HCN_2$ and the elimination TS lie at relative energies of −1.2 and 18.6 kcal mol^{-1} with respect to reactants at the CCSD(T)/cc-pVTZ//B3LYP/6-311G* level. The corresponding values with the cc-pVQZ basis set are, respectively, of −1.1 and 19.6 kcal mol^{-1}. This suggests an accuracy of *ca.* 1 kcal mol^{-1} for the key energetics, which is adequate for transition state theory at the high temperatures relevant for the kinetics of this reaction.

Note that for calculation of the MECP energetics at the CCSD(T) level, standard single-point energy calculations are not meaningful. The energies of the two states computed with one method at an MECP geometry optimized with another method are not necessarily degenerate. Instead, therefore, we have used the hybrid method suggested by us,[21] whereby the MECP is optimized using gradients calculated at the B3LYP level, and energies calculated using the CCSD(T) method. All geometries and energies are in reasonable agreement with those obtained in the previous high-level work.[47]

Next, we have applied non-adiabatic transition state theory in the formulation given above to calculate the thermal rate coefficient for the reaction as a function of temperature. At the MECP, we use a spin–orbit coupling matrix element of 10 cm^{-1} as in the previous work.[25]

Our transition state theory calculations take into account the role of the two TSs, the MECP, and the intermediates, using the unified statistical formalism of Miller[58] for multi-step processes. The overall number of reactive rovibrational states $N(E)$ for a given energy E is given by:

$$\frac{1}{N(E)} = \frac{1}{N_{TS1}(E)} - \frac{1}{N'_D(E)} + \frac{1}{N_{cr}(E)} - \frac{1}{N'_Q(E)} + \frac{1}{N_{TS2}(E)} \quad (7)$$

In this equation, $N_{TS1}(E)$ and $N_{TS2}(E)$ are the number of rovibrational states at TS1 and TS2, respectively, whereas $N_{cr}(E)$ is the effective number of states leading to surface hopping at the MECP, as given in eqn (1) above. $N'_D(E)$ and $N'_Q(E)$ are the number of rovibrational states calculated for the doublet and quartet HCN_2 minima, respectively, whilst omitting the vibrational degree of freedom corresponding to the reaction coordinate.[58] In this case, this corresponds to the NCN bending mode. Note that, because all the numbers of states in eqn (7) are calculated for the same total energy, the low energy of the HCN_2 minima on the potential energy surfaces means that $N'_D(E)$ and $N'_Q(E)$ are much larger than all the other terms, so that their reciprocals do not contribute significantly to the summation.

The overall thermal rate coefficient for reaction (6) is then computed using the Boltzmann averaging eqn (5). Note that the use of eqn (7) and (5) together involves the assumption that once the reactants HC and N_2 collide, they do not exchange

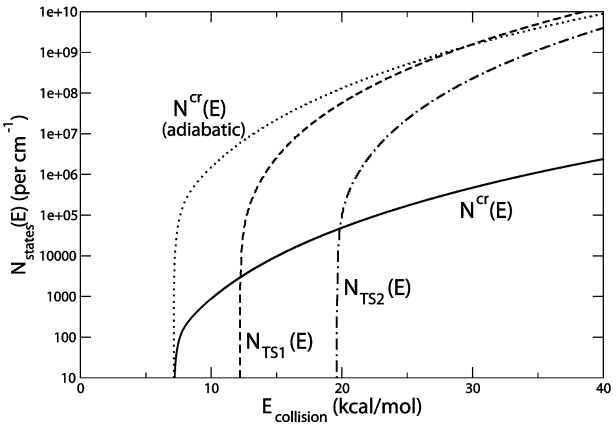

Fig. 6 Calculated number of states $N_{TS1}(E)$ at TS1, $N_{TS2}(E)$ at TS2, and $N_{cr}(E)$ at the MECP for the reaction HC + N_2, as a function of energy. Also shown is the number of states $N_{cr}(E)$ (adiabatic) at the MECP, calculated assuming unit probability for surface hopping p_{sh} in eqn (2).

any energy with the environment until the collisional complex either reverts to reactants or splits to form products. This assumption is justified given the fairly small bond energy of doublet and quartet HCN_2, the high temperature, and the relatively low density of states in these small tetraatomic species. At lower temperatures, as already mentioned, the linear isomer HCN_2 undergoes collisional cooling.

The calculated numbers of states entering into eqn (7) are shown in Fig. 6. As already mentioned, N'_D and N'_Q are larger than the other numbers of states at all energies, hence play no important role and are omitted from Fig. 6 for clarity. As can be seen on this logarithmic plot, the number of states at each critical point is zero below the relevant critical energy: 7.1 kcal mol^{-1} for the MECP, 12.2 kcal mol^{-1} for TS1, and 19.6 kcal mol^{-1} for TS2, and climbs steeply above this threshold. Had we allowed for tunneling through the MECP or the two TSs, the numbers of states functions would not have shown a sharp increase from zero at threshold, but would have increased slightly more smoothly. This would not change the overall results in a significant way.

It is interesting to note that $N_{TS1}(E)$ and $N_{TS2}(E)$ have a similar behaviour above threshold, in that translation along the energy scale would bring them into close overlap. This is because the two TSs have similar rotational constants and vibrational frequencies.[47] In fact, the curve for $N_{cr}(E)$ also has a similar shape but it would need to be translated *upwards* as well as horizontally in order to overlap the others. The value reached just above threshold for this effective number of states is of the order of 10–1000, *i.e.*, considerably smaller than the value reached for the number of states at the adiabatic TSs, which reach 10^4–10^6 very rapidly after their respective thresholds. The reason for this difference is that the probability of surface hopping p_{sh} plays an important role in defining $N_{cr}(E)$, see eqn (2), and this probability is fairly low for this system. Spin–orbit coupling of the doublet and quartet electronic wavefunctions for HCN_2 in the vicinity of the MECP is relatively small, so the system is very close to the diabatic limit.

The $N_{cr}(E)$ curve is nevertheless similar in shape to the other curves because the net contribution of p_{sh} in eqn (2) does not vary much with energy. This is, at first sight, surprising because the Landau–Zener expression (3) for $p_{sh}(E_h)$ does depend on the inverse of the square root of the energy in the mode orthogonal to the crossing seam. However, in eqn (2), the density of states in the modes orthogonal to the crossing seam, $\rho_{cr}(E - E_h)$, increases rapidly with energy, such that the convolution is dominated by the terms with E_h close to threshold. This means that $N_{cr}(E)$ is roughly given by the value it would take if crossing was adiabatic, ($N_{cr}(E)$ (adiabatic), given by eqn (2) with $p_{sh} = 1$), times an average, energy-independent, hopping probability $\langle p_{sh} \rangle$.

$$N_{cr}(E) \approx \langle p_{sh} \rangle \times N_{cr}(E) \text{ (adiabatic)} \qquad (8)$$

The function $N_{cr}(E)$ (adiabatic) is shown by the dotted line in Fig. 6. It has a shape similar to the other adiabatic number of state functions. The mean hopping probability $\langle p_{sh} \rangle$ is small, with a value of *ca.* 10^{-4}.

The effect of eqn (7) is that at each energy, the overall number of states $N(E)$, not shown in Fig. 2, is essentially given by whichever of the three functions $N_{TS1}(E)$, $N_{cr}(E)$ or $N_{TS2}(E)$ is smallest at that energy. Hence, below 19.6 kcal mol^{-1}, $N(E)$ is zero, as $N_{TS2}(E)$ is equal to zero. For a very small energy range above this threshold, $N(E)$ is roughly equal to $N_{TS2}(E)$. Above 19.8 kcal mol^{-1}, however, N_{cr} becomes smaller than N_{TS2} due to the small net hopping probability $\langle p_{sh} \rangle$.[59] This means that, except in a very small energy range above the overall reaction threshold, where the reaction probability is determined by the properties of TS2, the MECP plays a dominant role.

The corresponding thermal rate coefficient is given by eqn (5), and is shown as an Arrhenius plot in Fig. 7 together with the experimental data. Using the combined number of states function $N(E)$ of eqn (7) gives the $k_{overall}$ curve in Fig. 7. As can be seen, this lies well below the experimental curve, with a difference of *ca.* three orders of magnitude at the highest temperature of 4000 K. Also shown in Fig. 7 are the rate coefficients calculated by assuming that either TS2 or the surface-crossing at the MECP, respectively, represent the only bottleneck to reaction. These values can be obtained easily by inserting either $N_{TS2}(E)$ or $N_{cr}(E)$, respectively, in eqn (5), instead of the combined number of states function of eqn (7).[60] Within the range of temperatures relevant to the experiments (most measurements were carried out above 2000 K[49]), it can be seen that the overall calculated rate coefficient is very similar to $k_{cr}(T)$, and is much smaller than $k_{TS2}(T)$.

This behaviour follows quite naturally from the number of states plots of Fig. 6: N_{cr} is smaller than N_{TS2} at almost all relevant energies, and hence the MECP represents the main bottleneck to reaction.

At lower temperatures, $k_{overall}$ deviates quite significantly from k_{cr}, and this is because the Boltzmann weighting of eqn (5) favours lower energies much more at lower temperatures. At temperatures towards the right-hand side of Fig. 7, *i.e.* between 1000 and 2000 K, analysis of the data shows that both TS2 and the MECP play a role as bottlenecks to reaction. The average internal energy of systems undergoing reaction at 1000 K (based on the weighting eqn (5)) is 23.45 kcal mol^{-1},

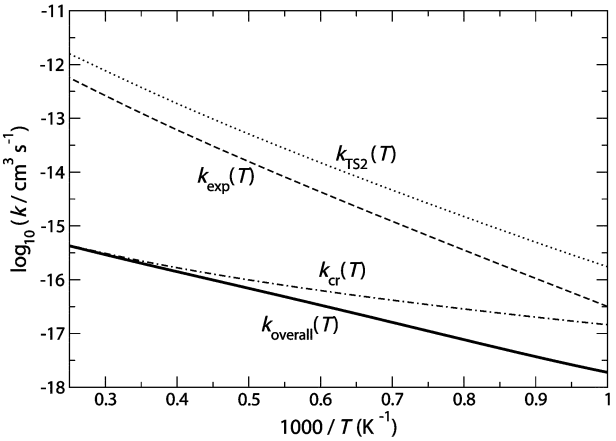

Fig. 7 Calculated and experimental[49] thermal rate coefficients $k(T)$ for the reaction of HC with N_2. The calculated curves k_{TS2}, k_{cr} and $k_{overall}$ are calculated using eqn (5), using $N(E)$ equal to $N_{TS2}(E)$, $N_{cr}(E)$ and $N(E)$ of eqn (6), respectively.

which would suggest that only the MECP plays the role of bottleneck, and indeed, $k_{overall}$ is closer to k_{cr} at that temperature than to k_{TS2}. However, this is the *average* energy, and a significant contribution to $k(T)$ will be made by systems below this energy, and for these, eqn (7) will make the overall rate constant smaller than it would be if the MECP was the *only* bottleneck to reaction.

At still lower temperatures (not shown in Fig. 7), $k_{overall}$ is very small, with TS2 acting as the main bottleneck to reaction. At 300 K, for example, k_{TS2} (1.3×10^{-26} cm^3 s^{-1}) is much smaller than k_{cr} (2.5×10^{-19} cm^3 s^{-1}), and $k_{overall}$ (1.4×10^{-27} cm^3 s^{-1}) is now determined largely by $N_{TS2}(E)$, with an average energy for reaction of 20.5 kcal mol^{-1}. At this low temperature, the Boltzmann factor in eqn (5) strongly favours reaction at energies just above threshold, where TS2 plays the dominant role.

In summary, at low temperatures close to room temperature, it is correct to argue that reactivity is dominated by systems undergoing collision with an internal energy just above threshold.[49] However, at the high temperatures of 2000 K and above, where most experimental work on this reaction has been carried out, this argument is incorrect. At 4000 K, the average energy of reaction is of 52 kcal mol^{-1}, and at these energies the low hopping probability at the MECP makes the latter a much more effective barrier to reaction than TS2.

Our calculated values of $k_{overall}$ are slightly larger (by a factor of 10 at 1000 K and a factor of 2 at 3000 K) than those derived by others previously using a similar form of non-adiabatic TST.[25,61] These relatively small differences can be expected due to slightly different features in the potential energy surfaces. The treatment of the hopping probability is also different, but this should not have a large impact on the calculated values. Like the previous study, our work shows that the rate of this reaction is strongly affected by its spin-forbidden nature.

The poor agreement between experiment and theory for the rate constant of reaction (6) is thereby yet again confirmed.[25,50,51] This is not due to errors in the theory, however. Indeed, the approximate non-adiabatic transition state theory yields results quite similar to those obtained from more accurate quantum scattering methods. Instead, it has been shown that the experimental data for reaction (5) does not correspond to formation of the products HCN + N. Instead, HC and N_2 can react in a spin-allowed way to form the NCN radical and an H atom.[62] The former species can rapidly generate NO in the presence of O_2, and calculated rate constants for this process are in quite good agreement with the experimental results. The alternative mechanism leading to HCN + N is genuinely "spin-forbidden", because it would compete with the process leading to NCN + H if the spin-state change did not need to occur.

Although the spin-forbidden process is not directly experimentally relevant, it has been discussed at some length here for two reasons. First, very accurate quantum dynamical calculations have been carried out on this reaction, and the good agreement between the non-adiabatic TST and more accurate calculations provides support for the accuracy of the former. Next, the reasons for which surface-crossing at the MECP is the dominant bottleneck for this reaction at the experimentally relevant temperatures are of considerable general interest for understanding the kinetics of spin-forbidden reactions, as discussed in Section 6 below.

5. Accuracy of non-adiabatic TST

As shown in the examples above, non-adiabatic TST[11–13] combined with an accurate determination of the properties of the MECP[14,15] yields reasonably accurate results for rate coefficients for a number of rather different reactions. Nevertheless, the results from this theory are by no means exact. The reasons for this have been discussed in some detail previously[14,15,25] and are only briefly summarized here.

One obvious source of inexact results is inaccuracy of the underlying computations concerning the potential energy surfaces and their coupling. The theory requires the rotational constants and vibrational frequencies of the reactants and the MECP. Also needed are the slopes of the two surfaces at the MECP, the magnitude of the spin–orbit coupling matrix element at the MECP, the reduced mass along the direction orthogonal to the crossing seam at the MECP, and the energy of the MECP relative to the reactants. By and large, the same level of accuracy is expected for these properties as in other *ab initio* calculations.

It should, however, be noted that the overall rate constant is very sensitive, especially at lower energies and temperatures, to the relative energy of the MECP, and hence the latter needs to be determined very accurately. As already pointed out in several previous publications,[15,21,63] this will not usually be possible if the chosen method is not able to reproduce the spin-state splitting, *i.e.*, the energy difference between stable species on the two potential energy surfaces. This means that accurate methods are often required when locating MECPs. For example, Hartree–Fock theory, which will often be adequate for predicting the geometry (if not the energy) of transition states for adiabatic reactions, may fail severely when predicting the properties of the MECP even in simple organic systems.[21] In

transition metal chemistry, it has become apparent in recent years that different DFT functionals sometimes predict very different spin-state splittings,[64,65] so that a particular functional may give poor results for the MECP energy in some systems.

Even with exact potential energy surfaces and couplings, however, the theory would not yield perfect results. This is partly a reflection of the fact that non-adiabatic TST makes many of the same approximations as normal TST. For example, the vibrational frequencies are treated as harmonic oscillators and the molecules and the MECP are treated as rigid rotors. Also, the reactants are assumed to move through phase space during vibrations and collisions in a statistical way. Finally, motion along the reaction coordinate (the direction orthogonal to the crossing seam) is assumed to be uncoupled from that in other degrees, at least in the region of the TS or MECP. None of these assumptions is strictly correct, which means that, at best, TST methods yield accuracy of the order of one order of magnitude. One approximation that is specific for non-adiabatic TST is the use of the approximate expressions (3) and (4) for the probability of hopping from one surface to another. Other expressions for this hopping probability have been suggested,[66] and in some cases exact one-dimensional solutions have been used.[25] In many cases, we find that results derived using eqn (3) and (4) are similar to within a factor of 2 or 3 at most, suggesting that the expression used to describe the hopping probability does not enormously affect the quality of the results obtained.

The approximation of independent motion in the reaction coordinate is worth discussing more carefully as its implications are different in normal TST and for spin-forbidden reactions. Concerted motion along several coordinates is particularly important because it can lead to enhanced tunneling due to so-called 'corner-cutting'. Within transition-state theory for adiabatic reactions, powerful algorithms have been developed to treat this effect.[67] The use of the hopping probability expression of eqn (4) does allow for some tunneling, but without any curvature. Also, this equation assumes that the potential energy surfaces are linear in the region of the MECP. In work by other authors on the HC + N_2 reaction,[25] a more accurate approach, analogous to the zero-curvature tunneling method for standard TST, has been used. The results are, however, similar to ours described here, suggesting that this more accurate expression does not give very different results for this case at least.

For this same reaction, accurate 2- and 3-dimensional quantum dynamical calculations have been carried out and compared to the results derived from a one-dimensional treatment of the surface crossing.[51] All three calculations include the effect of the remaining degrees of freedom using a convolution procedure similar to that of eqn (2). The more accurate 2- and 3-dimensional calculations do yield results that differ by approximately one order of magnitude from the more simple one-dimensional model, showing that the reaction coordinate does in fact couple to other degrees of freedom. This kind of discrepancy is expected to be most severe in cases where spin-forbidden reactions involve tunnelling at energies well below the MECP. Even for reactions at energies above the barrier, however, such many-dimensional effects may be important.

Nevertheless, we have observed for several cases that non-adiabatic TST yields results that are in good agreement with either more accurate theory or with experiment. Even where discrepancies have been found by others,[51] they are relatively small. This suggests that the method can yield results of semi-quantitative accuracy, perhaps to within one order of magnitude of experiment. This is not accurate enough for quantitative purposes, but it is enough to be able to provide insight into reactivity.

6. Kinetics of spin-forbidden reactions

Eqn (1) and (5) provide general expressions for the energy- and temperature-dependent rate coefficients of spin-forbidden reactions. In this section, we discuss the kinetic features of these reactions, and how they relate to the kinetics of spin-allowed reactions.

First, the kinetics of spin-forbidden reactions are to a large degree determined, as for any reaction, by the shape of the potential energy surfaces involved. In particular, the relative energy of the highest point along the energy profile will play a key role in determining reactivity. Locating an MECP for a given reaction allows one to determine the impact of the need to change spin-state.

However, the strength of spin–orbit coupling also plays an important role in determining reactivity. The surface-hopping probability is, in principle, energy-dependent but in practice nearly constant (eqn (8)). This means that the integrated density of states $N(E)$ and the energy-dependent rate constant $k(E)$ are given by some fraction $\langle p_{sh} \rangle$ of the values they would adopt for a reaction proceeding through an adiabatic transition state with the same relative energy and properties as the MECP. For the HC + N_2 reaction, $\langle p_{sh} \rangle$ is of the order of 0.0002.

Taking eqn (5) and (8) together, a similar expression can be given for the *thermal* rate constant of a reaction with a single rate-limiting step involving passing through an MECP:

$$k(T) \approx \langle p_{sh} \rangle \times k_{adiabatic}(T) \qquad (9)$$

In this equation, $k_{adiabatic}(T)$ is the hypothetical rate constant for the analogous spin-allowed reaction, and $\langle p_{sh} \rangle$ is the mean probability of surface-hopping, which as noted before is roughly energy-, and hence temperature-, independent. The reactions of CO with $Fe(CO)_4$ and the haem group, discussed above, are examples of spin-forbidden reactions involving only a single, spin-forbidden step. We have plotted $k(T)$ and $k_{adiabatic}(T)$ for these reactions,[15,45] and find that eqn (9) applies reasonably well across the temperature range. For example, in Fig. 4, the $k_{adiabatic}$ and $k_{spin\text{-}forbidden}$ curves are almost parallel. Note that as the $k_{adiabatic}$ values do not include a correction for tunneling, they should be compared for the present purposes to the $k_{spin\text{-}forbidden}$ values derived using eqn (3). For $Fe(CO)_4$ + CO,[15] where the spin–orbit coupling matrix element is 66 cm^{-1}, $\langle p_{sh} \rangle$ is *ca.* 0.05. For the reaction with the haem group,[45] where an estimated value of 10 cm^{-1} for the spin–orbit coupling matrix element was used, $\langle p_{sh} \rangle$ is *ca.* 0.003.

These values of $\langle p_{sh} \rangle$ should be fairly typical of a broad range of reactions. Depending on the strength of spin–orbit coupling, spin-forbidden reactions are thereby expected to be slower than analogous spin-allowed reactions by 1 to 4 orders of magnitude. At room temperature, this factor represents a significant but not prohibitive hindrance to reaction. To obtain a similar decrease in rate constant for an adiabatic reaction, it would be necessary to increase the barrier height by between 1.4 and 5.5 kcal mol^{-1}. This suggests that at room temperature, spin-forbidden reactions should be fairly common, given that in some cases at least, the relevant MECPs should lie somewhat lower than TSs for competing adiabatic pathways.

In contrast, at higher temperatures, a decrease in reactivity by 1 to 4 orders of magnitude is a more significant effect. At 2000 K, a $\langle p_{sh} \rangle$ of 10^{-4} has the same effect on the rate coefficient as an increase in the adiabatic barrier by 36 kcal mol^{-1}! This explains why the MECP represents the bottleneck for the reaction of HC with N_2 at higher temperatures, despite the fact that it lies so much lower in energy than TS2.

Eqn (9) can be expanded by inserting the TST expression for $k_{adiabatic}$. The mean hopping probability $\langle p_{sh} \rangle$ plays the same role in eqn (10) as the transmission probability in standard TST (as discussed in Section 5 above, other factors may also contribute to the transmission probability).

$$k(T) \approx \langle p_{sh} \rangle \times \frac{k_B T}{h} \exp\left(\frac{-\Delta G^{\ddagger}}{RT}\right) \qquad (10)$$

By expanding the activation free energy in eqn (10), one obtains eqn (11), in which temperature-dependent and independent terms have been regrouped:

$$k(T) = \frac{k_B T}{h} \exp\left(\frac{-\Delta H^{\ddagger}}{RT}\right) \times \langle p_{sh} \rangle \times \exp\left(\frac{\Delta S^{\ddagger}}{R}\right) \qquad (11)$$

This shows that $\langle p_{sh} \rangle$ plays the role of an additional contribution to the activation entropy. For example, a mean hopping probability of 0.003, as calculated for the reaction of CO with the haem group in myoglobin, is equivalent to a negative contribution to the entropy of activation of −11.5 cal mol^{-1} K^{-1}. The entropy of activation of this reaction[68] (−19.4 cal mol^{-1} K^{-1}) is indeed quite strongly negative, much more so than the analogous reaction with O_2 (−7.2 cal mol^{-1} K^{-1}). In general, spin-forbidden reactions can be expected to display unexpectedly low activation entropies, and this also explains why such processes do not compete effectively at high temperatures, where entropic effects tend to dominate over enthalpic ones.

7. Conclusions

Spin-forbidden reactions are an important class of non-adiabatic reaction. Such processes are fairly common in photochemistry but also in thermal chemistry. It is useful to have a general model to rationalize reactivity in such cases. The non-adiabatic form of transition state theory reviewed here performs well in terms of reproducing rate coefficients for a number of different spin-forbidden reactions. This theory also provides a useful model for assessing spin-forbidden reactivity in a more qualitative way and includes two important factors: the critical energy for reaction; and the surface-hopping probability. For spin-forbidden reactions, the critical energy is usually defined by the relative energy of the MECP for the considered reaction or reaction step. This relative energy has almost exactly the same effect on reactivity as the critical energy of the highest transition state for adiabatic reactions. The surface-hopping probability is mostly defined by the strength of spin–orbit coupling between the zeroth-order electronic wavefunctions of the two spin states in the vicinity of the MECP.

The reaction of HC with N_2 is an interesting case study of the relative importance of these two factors in determining reactivity. Formation of HCN + N requires the crossing of a number of adiabatic barriers, including a fairly high one in the exit channel lying 19.6 kcal mol^{-1} higher than reactants. It also requires passing through an MECP lying only 7.1 kcal mol^{-1} higher than reactants. At the high temperatures experimentally relevant for this reaction, the low surface-hopping probability at the MECP makes the spin-state change the key factor in determining reactivity, despite the much lower energy of the MECP compared to the adiabatic TS. The predicted rate coefficients for formation of HCN and N—which are in good agreement with those calculated using more accurate methods—are much smaller than the experimental rate coefficient for loss of reactants. This is because there is an alternative, spin-allowed mechanism leading to NCN + H that dominates over the spin-forbidden channel.

Analysis of the expressions given for the rate coefficients of spin-forbidden reactions, as well as of the results of actual calculations, suggests some general trends for the kinetic behaviour of this class of reaction. First, it can be seen that spin-forbidden reactions should behave in a roughly similar way to analogous spin-allowed reactions. Eqn (10) and (11) show that their rate is given by an extended Eyring equation, at least in simple cases in which there is only one kinetically important reaction step, and this is the spin-forbidden step. This means that for these cases, plots of $\ln(k)$ or of $\ln(k/T)$ *versus* $(1/T)$ should be roughly linear, with their slope defined by the critical energy for reaction. In turn, this critical energy for reaction will be defined by the relative energy of the MECP.

The main difference with respect to the analogous spin-allowed reactions is the presence of the $\langle p_{sh} \rangle$ factor measuring the mean surface hopping probability. Where spin–orbit coupling between the electronic wavefunctions is very small, $\langle p_{sh} \rangle$ can also be very small. This has the effect of introducing an additional unfavourable contribution to the activation entropy of the reaction, meaning that spin-forbidden reactions will compete with spin-allowed reactions involving similar barrier heights quite effectively at lower temperatures or energies, but much less so at higher temperatures.

The accuracy of the model discussed in the present paper has still only been tested for a fairly small number of cases, and it would clearly be desirable to make comparisons with experiment or more accurate theory for many more cases. More experience will also help chemists to use the theory in an informal way to predict reactivity in a wide range of

spin-forbidden reactions, in the same way as standard transition state theory is used for adiabatic reactions.

Acknowledgements

The author thanks Massimiliano Aschi, Rinaldo Poli, Detlef Schröder, Mike George, Nikola Strickland and José-Luis Carreón-Macedo for many helpful discussions on spin-forbidden reactions and theory. The award of an Advanced Research Fellowship from EPSRC is also acknowledged.

References

1 S. C. Althorpe and D. C. Clary, *Annu. Rev. Phys. Chem.*, 2003, **54**, 493–529.
2 B. Kerkeni and D. C. Clary, *Phys. Chem. Chem. Phys.*, 2006, **8**, 917–925.
3 T. Wu, H.-J. Werner and U. Manthe, *Science*, 2004, **306**, 2227–2229.
4 D. G. Truhlar, B. C. Garrett and S. J. Klippenstein, *J. Phys. Chem.*, 1996, **100**, 12771–12800.
5 F. Claeyssens, J. N. Harvey, F. R. Manby, R. A. Mata, A. J. Mulholland, K. E. Ranaghan, M. Schütz, S. Thiel, W. Thiel and H.-J. Werner, *Angew. Chem., Int. Ed.*, 2006, **45**, 6856–6859.
6 L. Masgrau, A. Roujeinikova, L. O. Johannissen, P. Hothi, J. Basran, K. E. Ranaghan, A. J. Mulholland, M. J. Sutcliffe, N. S. Scrutton and D. Leys, *Science*, 2006, **312**, 237–241.
7 See *e.g.* P. J. Lewis, K. Bennett and J. N. Harvey, *Phys. Chem. Chem. Phys.*, 2005, **7**, 1643–1649.
8 (*a*) P. Hänggi, P. Talkner and M. Borkovec, *Rev. Mod. Phys.*, 1990, **62**, 251–341; (*b*) B. K. Carpenter, *Annu. Rev. Phys. Chem.*, 2005, **56**, 57–89.
9 (*a*) For previous reviews from our group relating to spin-forbidden reactions, see: J. N. Harvey, in *Computational Organometallic Chemistry*, ed. T. R. Cundari, Marcel Dekker, New York, Basel, 2001; (*b*) J. N. Harvey, R. Poli and K. M. Smith, *Coord. Chem. Rev.*, 2003, **238–239**, 347–361; (*c*) R. Poli and J. N. Harvey, *Chem. Soc. Rev.*, 2003, **32**, 1–8.
10 For previous reviews from other groups concerning spin-forbidden reactions, see: (*a*) P. J. Dagdigian and M. L. Campbell, *Chem. Rev.*, 1987, **87**, 1–18; (*b*) R. Poli, *Acc. Chem. Res.*, 1997, **30**, 494–501; (*c*) D. A. Plattner, *Angew. Chem., Int. Ed.*, 1999, **38**, 82–86; (*d*) D. Schröder, S. Shaik and H. Schwarz, *Acc. Chem. Res.*, 2000, **33**, 139–145; (*e*) P. Gütlich, Y. Garcia and H. A. Goodwin, *Chem. Soc. Rev.*, 2000, **29**, 419–427; (*f*) R. Poli, *J. Organomet. Chem.*, 2004, **689**, 4291–4304; (*g*) H. Schwarz, *Int. J. Mass Spec.*, 2004, **237**, 75–105; (*h*) B. K. Carpenter, *Chem. Soc. Rev.*, 2006, **35**, 736–747.
11 J. B. Delos, *J. Chem. Phys.*, 1973, **59**, 2365–2369.
12 (*a*) J. C. Tully, *J. Chem. Phys.*, 1974, **61**, 61–68; (*b*) G. E. Zahr, R. K. Preston and W. H. Miller, *J. Chem. Phys.*, 1975, **62**, 1127–1135.
13 J. C. Lorquet and B. Leyh-Nihant, *J. Phys. Chem.*, 1988, **92**, 4778–4783.
14 J. N. Harvey and M. Aschi, *Phys. Chem. Chem. Phys.*, 1999, **1**, 5555–5563.
15 J. N. Harvey and M. Aschi, *Faraday Discuss.*, 2003, **124**, 129–143.
16 C. Zener, *Proc. R. Soc. London, Ser. A*, 1932, **137**, 696–702.
17 (*a*) E. E. Nikitin, *Annu. Rev. Phys. Chem.*, 1999, **50**, 1–21; (*b*) C. Wittig, *J. Phys. Chem. B*, 2005, **109**, 8428–8430, and refs. therein.
18 Here too, the energy argument should be $E_h - E_c$. Also, the minus sign in the Airy function was mistakenly omitted in two of our earlier papers (ref. 14 and 15) but is correctly given *e.g.*, in ref. 11 and 13.
19 The MECP is not a conical intersection because, in general, the spin–orbit coupling element H_{12} will be non-zero and hence will lift the degeneracy of the two diabatic surfaces. It is of course possible that H_{12} will vary within the crossing seam, and may indeed become zero in places, which will define a true conical intersection between adiabatic surfaces.
20 M. J. Bearpark, M. A. Robb and H. B. Schlegel, *Chem. Phys. Lett.*, 1994, **223**, 269–274.
21 J. N. Harvey, M. Aschi, H. Schwarz and W. Koch, *Theor. Chem. Acc.*, 1998, **99**, 95–99.
22 (*a*) N. Koga and K. Morokuma, *Chem. Phys. Lett.*, 1985, **119**, 371–374; (*b*) A. Farazdel and M. Dupuis, *J. Comput. Chem.*, 1991, **12**, 276–282; (*c*) D. R. Yarkony, *J. Phys. Chem.*, 1993, **97**, 4407–4412; (*d*) L. De Vico, M. Olivucci and R. Lindh, *J. Chem. Theory Comput.*, 2005, **1**, 1029–1037.
23 K. M. Smith, R. Poli and J. N. Harvey, *New J. Chem.*, 2000, **24**, 77–80.
24 Note that this is not true for the related non-adiabatic problem of locating conical intersections. In such cases, non-adiabatic coupling terms of the form $\langle\Psi|\partial\Psi/\partial R\rangle$ are required, and these cannot readily be computed using *e.g.*, the DFT methods used in our studies of MECPs. Also, in the vicinity of the conical intersection, the adiabatic wavefunctions will often have very high multi-reference character that again requires the use of MCSCF or MR-CI methods.
25 Q. Cui, K. Morokuma, J. M. Bowman and S. J. Klippenstein, *J. Chem. Phys.*, 1999, **110**, 9469–9482.
26 (*a*) E. L. Øiestad, J. N. Harvey and E. Uggerud, *J. Phys. Chem. A*, 2000, **104**, 8382–8388; (*b*) M. Aschi and J. N. Harvey, *J. Chem. Soc., Perkin Trans. 2*, 1999, 1059–1062; (*c*) D. Schröder, C. Heinemann, H. Schwarz, J. N. Harvey, S. Dua, S. Blanksby and J. H. Bowie, *Chem.–Eur. J.*, 1998, **4**, 2550–2557; (*d*) C. A. Schalley, J. N. Harvey, D. Schröder and H. Schwarz, *J. Phys. Chem. A*, 1998, **102**, 1021–1035.
27 (*a*) J.-L. Carreón-Macedo, J. N. Harvey and R. Poli, *Eur. J. Inorg. Chem.*, 2005, **1**, 2999–3008; (*b*) J.-L. Carreón-Macedo and J. N. Harvey, *J. Am. Chem. Soc.*, 2004, **126**, 5789–5797.
28 M. E. Lundberg and P. E. M. Siegbahn, *Chem. Phys. Lett.*, 2005, **401**, 347–351.
29 D. W. Keogh and R. Poli, *J. Am. Chem. Soc.*, 1997, **119**, 2516–2523.
30 Among work by other groups using similar or related spin-forbidden transition state theories and not cited below, see: *e.g.*, (*a*) M. Aschi and F. Grandinetti, *J. Chem. Phys.*, 1999, **111**, 6759–6768; (*b*) A. J. Marks, *J. Chem. Phys.*, 2001, **114**, 1700–1708; (*c*) M. Aschi and A. Largo, *Chem. Phys.*, 2001, **265**, 251–261; (*d*) N. E. Henriksen and F. Y. Hansen, *Phys. Chem. Chem. Phys.*, 2002, **4**, 5995–6000; (*e*) Y. Zhao, G. Mil'nikov and H. Nakamura, *J. Chem. Phys.*, 2004, **121**, 8854–8860; (*f*) A. Cimas, V. M. Rayón, M. Aschi, C. Barrientos, J. A. Sordo and A. Largo, *J. Chem. Phys.*, 2005, **123**, 114312; (*g*) Y. Zhao, X. Li, Z. Zheng and W. Liang, *J. Chem. Phys.*, 2006, **124**, 114508.
31 A. J. Marks and D. L. Thompson, *J. Chem. Phys.*, 1992, **96**, 1911–1918.
32 A. H. H. Chang and D. R. Yarkony, *J. Chem. Phys.*, 1993, **99**, 6824–6831.
33 H. Nakamura and S. Kato, *J. Chem. Phys.*, 1999, **110**, 9937–9947.
34 M. Aschi, J. N. Harvey, C. A. Schalley, D. Schröder and H. Schwarz, *Chem. Commun.*, 1998, 531–532.
35 One of these MECPs was also described earlier D. R. Yarkony, *J. Am. Chem. Soc.*, 1992, **114**, 5406–5411.
36 M. M. Bursey, J. R. Hass, D. J. Harvan and C. E. Parker, *J. Am. Chem. Soc.*, 1979, **101**, 5485–5489.
37 See: *e.g.*, M. Merchán, L. Serrano-Andrés, M. A. Robb and L. Blancafort, *J. Am. Chem. Soc.*, 2005, **127**, 1820–1825.
38 A. J. G. Barwise, A. A. Gorman and M. A. J. Rodgers, *Chem. Phys. Lett.*, 1976, **38**, 313–316.
39 J. N. Harvey, S. Grimme, M. Woeller, S. D. Peyerimhoff, D. Danovich and S. Shaik, *Chem. Phys. Lett.*, 2000, **322**, 358–362.
40 (*a*) T. A. Seder, A. J. Ouderkirk and E. Weitz, *J. Chem. Phys.*, 1986, **85**, 1977–1986; (*b*) R. J. Ryther and E. Weitz, *J. Phys. Chem.*, 1991, **95**, 9841–9852; (*c*) E. Weitz, *J. Phys. Chem.*, 1994, **98**, 11256–11264; (*d*) J. Wang, J. T. Long and E. Weitz, *J. Phys. Chem. A*, 2001, **105**, 3765–3772.
41 P. T. Snee, C. K. Payne, S. D. Mebane, K. T. Kotz and C. B. Harris, *J. Am. Chem. Soc.*, 2001, **123**, 6909–6915.
42 P. Portius, J. Yang, X.-Z. Sung, D. C. Grills, P. Matousek, A. W. Parker, M. Towrie and M. W. George, *J. Am. Chem. Soc.*, 2004, **126**, 10713–10720.
43 J.-L. Carreón-Macedo and J. N. Harvey, *Phys. Chem. Chem. Phys.*, 2006, **8**, 93–100.

44 J. N. Harvey, *J. Am. Chem. Soc.*, 2000, **122**, 12401–12402.
45 J. N. Harvey, *Faraday Discuss.*, 2004, **127**, 165–177.
46 P. J. Steinbach, A. Ansari, J. Berendzen, D. Braunstein, K. Chu, B. R. Cowen, D. Ehrenstein, H. Frauenfelder, J. B. Johnson, D. C. Lamb, S. Luck, J. R. Mourant, G. U. Nienhaus, P. Ormos, R. Philipp, A. H. Xie and R. D. Young, *Biochemistry*, 1991, **30**, 3988–4001.
47 (*a*) M. R. Manaa and D. R. Yarkony, *J. Chem. Phys.*, 1991, **95**, 1808–1816; (*b*) J. M. L. Martin and P. R. Taylor, *Chem. Phys. Lett.*, 1993, **209**, 143–150; (*c*) T. Seideman and S. P Walch, *J. Chem. Phys.*, 1994, **101**, 3656–3661; (*d*) T. Takayanagi, *Chem. Phys. Lett.*, 2003, **368**, 393–398.
48 Q. Cui and K. Morokuma, *Theor. Chem. Acc.*, 1999, **102**, 127–133.
49 J. A. Miller and S. P. Walch, *Int. J. Chem. Kinet.*, 1997, **29**, 253–259.
50 T. Seideman, *J. Chem. Phys.*, 1994, **101**, 3662–3670.
51 A. Wada and T. Takayanagi, *J. Chem. Phys.*, 2002, **116**, 7065–7072.
52 A. D. Becke, *J. Chem. Phys.*, 1993, **98**, 5648–5652.
53 M. J. Frisch, J. A. Pople and J. S. Binkley, *J. Chem. Phys.*, 1984, **80**, 3265–3269.
54 M. J. Frisch, G. W. Trucks, H. B. Schlegel, G. E. Scuseria, M. A. Robb, J. R. Cheeseman, J. A. Montgomery, Jr., T. Vreven, K. N. Kudin, J. C. Burant, J. M. Millam, S. S. Iyengar, J. Tomasi, V. Barone, B. Mennucci, M. Cossi, G. Scalmani, N. Rega, G. A. Petersson, H. Nakatsuji, M. Hada, M. Ehara, K. Toyota, R. Fukuda, J. Hasegawa, M. Ishida, T. Nakajima, Y. Honda, O. Kitao, H. Nakai, M. Klene, X. Li, J. E. Knox, H. P. Hratchian, J. B. Cross, V. Bakken, C. Adamo, J. Jaramillo, R. Gomperts, R. E. Stratmann, O. Yazyev, A. J. Austin, R. Cammi, C. Pomelli, J. Ochterski, P. Y. Ayala, K. Morokuma, G. A. Voth, P. Salvador, J. J. Dannenberg, V. G. Zakrzewski, S. Dapprich, A. D. Daniels, M. C. Strain, O. Farkas, D. K. Malick, A. D. Rabuck, K. Raghavachari, J. B. Foresman, J. V. Ortiz, Q. Cui, A. G. Baboul, S. Clifford, J. Cioslowski, B. B. Stefanov, G. Liu, A. Liashenko, P. Piskorz, I. Komaromi, R. L. Martin, D. J. Fox, T. Keith, M. A. Al-Laham, C. Y. Peng, A. Nanayakkara, M. Challacombe, P. M. W. Gill, B. G. Johnson, W. Chen, M. W. Wong, C. Gonzalez and J. A. Pople, *GAUSSIAN 03 (Revision B.04)*, Gaussian, Inc., Wallingford, CT, 2004.
55 (*a*) P. J. Knowles, C. Hampel and H.-J. Werner, *J. Chem. Phys.*, 1993, **99**, 5219–5227; (*b*) Erratum P. J. Knowles, C. Hampel and H.-J. Werner, *J. Chem. Phys.*, 2000, **112**, 3106–3107.
56 R. D. Amos, A. Bernhardsson, A. Berning, P. Celani, D. L. Cooper, M. J. O. Deegan, A. J. Dobbyn, F. Eckert, C. Hampel, G. Hetzer, P. J. Knowles, T. Korona, R. Lindh, A. W. Lloyd, S. J. McNicholas, F. R. Manby, W. Meyer, M. E. Mura, A. Nicklass, P. Palmieri, R. Pitzer, G. Rauhut, M. Schütz, U. Schumann, H. Stoll, A. J. Stone, R. Tarroni, T. Thorsteinsson and H.-J. Werner, *MOLPRO, a package of ab initio programs designed by H.-J. Werner and P. J. Knowles, Version 2002.1*, 2002.
57 T. H. Dunning, Jr, *J. Chem. Phys.*, 1989, **90**, 1007–1022.
58 W. H. Miller, *J. Chem. Phys.*, 1976, **65**, 2216–2223.
59 In fact, in the very small energy range where $N_{TS2}(E)$ and $N^{er}(E)$ are similar, $N(E)$ will smoothly change from following one curve to the other, but this does not change the discussion.
60 The rate coefficient $k_{TS2}(T)$ can also be calculated using standard adiabatic TST, as was performed *e.g.* in ref. 49. Using our calculated properties for the reactants and TS2, the values of $k_{TS2}(T)$ calculated using $N_{TS2}(E)$ and eqn (5), and using standard TST are identical to within a few percent.
61 The rate coefficients in ref. 25 are given in graphical form as the curve $k_1(T)$ in Fig. 3d, in the units $cm^3\ mol^{-1}\ s^{-1}$. The rough values read off the graph and converted to $cm^3\ s^{-1}$ units are, respectively 1.7×10^{-19}, 1.7×10^{-17} and $1.3 \times 10^{-16}\ cm^3\ s^{-1}$ at 1020, 1850 and 3000 K. For comparison, we get values of 1.75×10^{-18}, 5.1×10^{-17} and $2.29\ 10^{-16}\ cm^3\ s^{-1}$ at these temperatures.
62 (*a*) L. V. Moskaleva, W. S. Xia and M. C. Lin, *Chem. Phys. Lett.*, 2000, **331**, 269–277; (*b*) G. P. Smith, *Chem. Phys. Lett.*, 2003, **367**, 541–548; (*c*) T. Takayanagi, *Chem. Phys. Lett.*, 2003, **368**, 393–398.
63 J.-L. Carreón-Macedo and J. N. Harvey, *Phys. Chem. Chem. Phys.*, 2006, **8**, 93–100.
64 (*a*) M. Reiher, O. Salomon and B. A. Hess, *Theor. Chem. Acc.*, 2001, **107**, 48–55; (*b*) O. Salomon, M. Reiher and B. A. Hess, *J. Chem. Phys.*, 2002, **117**, 4729–4737.
65 (*a*) J. N. Harvey, *Struct. Bonding*, 2004, **112**, 151–183; (*b*) J. N. Harvey, *Annu. Rep. Prog. Chem., Sect. C: Phys. Chem.*, 2006, **102**, 203–226.
66 See *e.g.* (*a*) C. Zhu and H. Nakamura, *J. Chem. Phys.*, 1994, **101**, 10630–10647; (*b*) C. Zhu and S. H. Lin, *J. Chem. Phys.*, 2006, **125**, 044104.
67 See *e.g.* (*a*) A. Chakraborty, Y. Zhao, H. Lin and D. G. Truhlar, *J. Chem. Phys.*, 2006, **124**, 044315; (*b*) Y.-P. Liu, D.-H. Lu, A. Gonzalez-Lafont, D. G. Truhlar and B. C. Garrett, *J. Am. Chem. Soc.*, 1993, **115**, 7806–7817.
68 H.-D. Projahn and R. van Eldik, *Inorg. Chem.*, 1991, **30**, 3288–3293.